Bis(alkylamino)phosphanes: Deprotonation Reactions and Reactivity of *t*-BuP(NH-*t*-Bu)$_2$ toward Group 13 Metalloorganics

Tillmann Bauer, Stephan Schulz,* Martin Nieger, and Ulrich Kessler

Institut für Anorganische Chemie, Universität Bonn, Gerhard-Domagk-Strasse 1, D-53121 Bonn, Germany

Received March 11, 2003

Reactions of the bis(amino)phosphane *t*-BuP(NH-*t*-Bu)$_2$ with base-stabilized alanes H_3Al-NR_3 occurred at the "hard" N center with elimination of dihydrogen, yielding [*t*-BuP(NH-*t*-Bu)N(*t*-Bu)AlH_2]$_2$ (**1**), whereas those with boranes, gallanes, and indanes MR_3 (M = B, Ga, In) took place at the "weak" P center, yielding the corresponding phosphane adducts *t*-Bu(NH-*t*-Bu)$_2$P-MR_3 (MR_3 = BH_3 (**2**), GaH_3 (**3**), $GaMe_3$ (**4**), $InMe_3$ (**5**)). A deprotonation reaction in Et_2O using an equimolar amount of *n*-BuLi resulted in the formation of the Li amidophosphane [*t*-BuP(NH-*t*-Bu)N(*t*-Bu)Li]$_2$ (**6**). **6** adopted a dimeric structure in the solid state but can be converted into its monomeric form by addition of tetramethylethylenediamine (tmeda), yielding *t*-BuP(NH-*t*-Bu)N(*t*-Bu)Li(tmeda) (**7**). It is also possible to prepare **7** by a deprotonation reaction with *n*-BuLi in tmeda. **6** was reacted with $GaCl_3$ with elimination of LiCl and formation of [*t*-BuP(NH-*t*-Bu)N(*t*-Bu)$GaCl_2$]$_x$ (**8**). Compounds **1**−**8** were investigated by means of (multinuclear) NMR (^{1}H, ^{13}C, ^{31}P, ^{7}Li) and IR spectroscopy. In addition, the crystal structures of [*t*-BuP(NH-*t*-Bu)N(*t*-Bu)AlH_2]$_2$ (**1**), *t*-Bu(NH-*t*-Bu)$_2$P−GaH_3 (**3**), [*t*-BuP-(NH-*t*-Bu)N(*t*-Bu)Li]$_2$ (**6**), and *t*-BuP(NH-*t*-Bu)N(*t*-Bu)Li(tmeda) (**7**) were determined by single-crystal X-ray diffraction.

Introduction

Aminophosphanes $R_xP(NR'_2)_{3-x}$ (x = 0−3) have a longstanding history in main-group-element chemistry,[1] in particular (dialkylamino)phosphanes of the types $RP(NR'_2)_2$ and $R_2PNR'_2$. They have been synthesized in large numbers, and their reactivity has been studied in detail due to the presence of both hard (N) and soft (P) Lewis basic centers (HSAB principle). In contrast, (alkylamino)phosphanes $R_xP(NHR)_{3-x}$ (x = 0,[2] 1,[3] 2[4]) and aminophosphanes $R_xP(NH_2)_{3-x}$ (x = 1,[5] 2[6]) have been investigated to a much lesser extent, due to their decreased stability with respect to consecutive condensation reactions. This tendency significantly increases with an increasing number of amino substituents and decreasing steric demand of the organic substituents, consequently reaching its maximum instability with tris(amino)phosphane, $P(NH_2)_3$. Pure $P(NH_2)_3$ has not yet been isolated in its pure form; however, it was stabilized as a BH_3 complex[7] or as a metal carbonyl complex.[8] The same approach was also used for P(NHR)$_3$.[9] As a result, most studies performed to date have dealt with the more stable monosubstituted (alkylamino)phosphanes R_2PNHR'. The interest in the synthesis of bis- and tris(amino)phosphanes has substantially increased only in the past decade, since their N−H functionality renders them as very promising building blocks for the preparation of novel substances or material classes. In particular, deprotonation reactions, leading to the novel imidophosphane anions $RP(NR'Li)_2$ as was shown recently by Nöth et al.,[10] are of great interest, since Li salts generally can act as starting

* To whom correspondence should be addressed. Phone: +49 (0)-228 73-5326. Fax: +49 (0)228 73-5327. E-mail: sschulz@uni-bonn.de.

(1) Initial reports go back to the early studies of Michaelis: (a) Michaelis, A.; von Soden, H. *Ann. Chem.* **1885**, *229*, 334. (b) Michaelis, A.; Schulze, G. *Chem. Ber.* **1893**, *26*, 2937. (c) Michaelis, A.; Schulze, G. *Chem. Ber.* **1894**, *27*, 2572. (d) Michaelis, A.; Luxembourg, K. *Chem. Ber.* **1895**, *28*, 2205.

(2) (a) Tarassoli, A.; Haltiwanger, R. C.; Norman, A. D. *Inorg. Nucl. Chem. Lett.* **1980**, *16*, 27. (b) Tarassoli, A.; Haltiwanger, R. C.; Norman, A. D. *Inorg. Chem.* **1982**, *21*, 2684.

(3) (a) Hitchcock, P. B.; Jasim, H. A.; Lappert, M. F.; Williams, H. D. *J. Chem. Soc., Chem. Commun.* **1986**, 1634. (b) Ahlemann, J.-T.; Roesky, H. W.; Murugavel, R.; Parisini, E.; Noltemeyer, M.; Schmidt, H.-G.; Müller, O.; Herbst-Irmer, R.; Markovskii, L. N.; Shermolovich, Y. G. *Chem. Ber.* **1997**, *130*, 1113.

(4) See for instance: (a) Aucott, S. M.; Slawin, A. M. Z.; Woollins, J. D. *J. Chem. Soc., Dalton Trans.* **2000**. 2559. (b) Wetzel, T. G.; Dehnen, S.; Roesky, P. W. *Angew. Chem., Int. Ed.* **1999**, *38*, 1086. (c) Kotov, V. V.; Avtomonov, E. V.; Sundermeyer, J.; Harms, K.; Lemenovskii, D. A. *Eur. J. Inorg. Chem.* **2002**, 678. (d) Poetschke, N.; Nieger, M.; Khan, M. A.; Niecke, E.; Ashby, M. T. *Inorg. Chem.* **1997**, *36*, 4087. (e) Kuhl, O.; Blaurock, S.; Sieler, J.; Hey-Hawkins, E. *Polyhedron* **2001**, *20*, 111. (f) Florke, U.; Haupt, H.-J. *Z. Kristallogr.* **1993**, *205*, 127.

(5) Scherer, O. J.; Klusmann, P. *Angew. Chem., Int. Ed. Engl.* **1968**, *7*, 560.

(6) (a) Scherer, O. J.; Klusmann, P. *Z. Anorg. Allg. Chem.* **1969**, *370*, 171. (b) Schick, G.; Loew, A.; Nieger, M.; Airola, K.; Niecke, E. *Chem. Ber.* **1996**, *129*, 911.

(7) (a) Kodama, A.; Parry, R. W. *J. Inorg. Nucl. Chem.* **1961**, *17*, 125. (b) Nordman, C. E. *Acta Crystallogr.* **1960**, *13*, 535.

(8) (a) Nöth, H.; Reith, H.; Thorn, V. *J. Organomet. Chem.* **1978**, *159*, 165. (b) Gieren, A.; Ruiz-Pérez, F. C.; Hübner, T.; Herberhold, M.; Schamel, K.; Guldner, K. *J. Organomet. Chem.* **1989**, *366*, 105. (c) Wrackmeyer, B.; Schamel, K.; Herberhold, M. *Z. Naturforsch.* **1989**, *44b*, 55.

(9) (a) Tarassoli, A.; Chen, H.-J.; Allured, V. S.; Hill, T. G.; Haltiwanger, R. C.; Thompson, M. L.; Norman, A. D. *Inorg. Chem.* **1986**, *25*, 3541. (b) Chen, H.-J.; Tarassoli, A.; Allured, V. S.; Haltiwanger, R. C.; Norman, A. D. *J. Organomet. Chem.* **1986**, *306*, C19. (c) Balashev, K. P.; Engebretsen, T.; Kvam, P.-I.; Maartmann-Moe, K.; Puzyk, M. V.; Songstad, J. *Acta Chem. Scand.* **1986**, *50*, 1108.

(10) Eichhorn, B.; Nöth, H.; Seifert, T. *Eur. J. Inorg. Chem.* **1999**, 2355.

10.1021/om0301839 CCC: $25.00
Publication on Web 06/20/2003

Chart 1. Products Obtained from Aminophosphane Reactions with Alanes

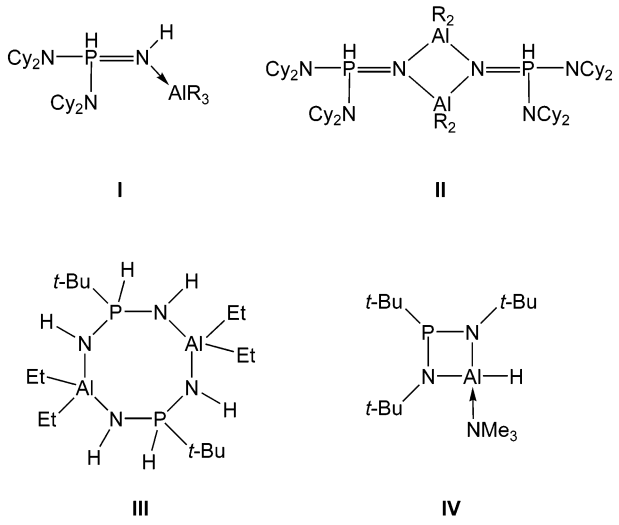

I II III IV

reagents for the introduction of a variety of p-, d-, and f-block elements to the P−N moiety. In addition, the electronic and structural similarities between imido and oxo anions of p-block elements has been the subject of intense study in recent years.[11]

We started working with aminophosphanes and (alkylamino)phosphanes due to our interest in the synthesis of elementorganic group 13/15 compounds containing an MNP backbone (M = Al, Ga, In). They are potential molecular *single-source precursors* for the preparation of ternary MNP materials. We focused on reactions with alanes of the types AlH_3, R_2AlH, and R_3Al in order to obtain molecular compounds containing an AlNP backbone. Reactions of bis(dicyclohexylamino)aminophosphane, $(Cy_2N)_2PNH_2$, with dialkyl- and trialkylalanes resulted in the formation of Lewis acid−Lewis base adducts $(Cy_2N)_2P(H)N(H)-AlR_3$ (**I**; Chart 1) and dimeric heterocycles of the type $[(Cy_2N)_2P(H)NAlR_2]_2$ (**II**),[12] whereas the reaction of *t*-$BuP(NH_2)_2$ with Et_2AlH yielded the eight-membered heterocycle [*t*-Bu(H)P-$(NH)_2AlEt_2]_2$ (**III**). **III** is the first example of a molecular aluminonitridophosphinate.[13] Consistently, each reaction of the aminophosphanes led to the formation of the thermodynamically favored iminophosphorane moiety (P−H form), as a result of the high Lewis acidity of the alane fragments.[14] In sharp contrast, reactions of the bis(alkylamino)phosphane *t*-BuP(NH-*t*-Bu)$_2$ with alanes (AlH_3,[15] AlR_3, R_2AlH[16]) did not occur with formation of the P−H form but with preservation of the N−H form. These studies finally led to the synthesis of the first neutral heterocyclic 1,3,2,4-diazaphosphaaluminatidine *t*-BuP(μ-N-*t*-Bu)$_2$AlH(NMe_3) (**IV**), which was characterized by single-crystal X-ray diffraction.

(11) For recent reviews see: (a) Brask, J. K.; Chivers, T. *Angew. Chem., Int. Ed.* **2001**, *40*, 3960. (b) Steiner, A.; Zacchini, S.; Richards, P. *Coord. Chem. Rev.* **2002**, *227*, 193. (c) Aspinall, G. M.; Copsey, M. C.; Leedham, A. P.; Russell, C. A. *Coord. Chem. Rev.* **2002**, *227*, 217.

(12) Schulz, S.; Raab, M.; Nieger, M.; Niecke, E. *Organometallics* **2000**, *19*, 2616.

(13) Schulz, S.; Bauer, T.; Nieger, M.; Krossing, I. *Chem. Commun.* **2002**, 1422.

(14) See the following and references therein: Raab, M.; Sundermann, A.; Schick, G.; Loew, A.; Nieger, M.; Schoeller, W. W.; Niecke, E. *Organometallics* **2001**, *20*, 1770.

(15) Schulz, S.; Bauer, T.; Nieger, M. *Chem. Commun.* **1999**, 879.

(16) Bauer, T.; Schulz, S.; Nieger, M. *Z. Anorg. Allg. Chem.* **2001**, *627*, 266.

Chart 2. Intra- versus Intermolecularly Stabilized Bis(amino)phosphanyl Alanes

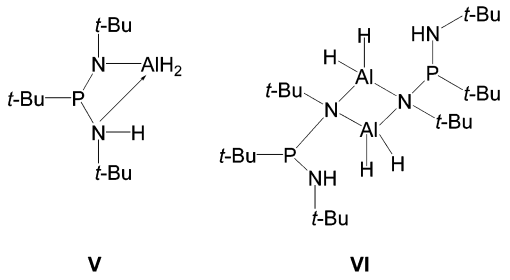

V VI

The promising results obtained from reactions of *t*-BuP(NH-*t*-Bu)$_2$ with alanes directed our interest toward reactions of bis(amino)phosphanes with other group 13 element compounds. Consequently, we performed reactions of *t*-BuP(NH-*t*-Bu)$_2$ with boranes, gallanes, and indanes. We also reinvestigated its reaction with the base-stabilized alanes H_3Al-NR_3 (NR_3 = NMe_3, NMe_2Et) in an attempt to obtain detailed structural information on the first reaction product. In addition, we studied deprotonation reactions using *n*-BuLi in order to generate synthetically valuable Li salts, which are expected to be stronger nucleophiles than the parent bis(amino)phosphane.

Results and Discussion

The equimolar reaction of pure *t*-BuP(NH-*t*-Bu)$_2$ and H_3Al-NR_3 at elevated temperature (120 °C) yielded the Lewis base stabilized four-membered heterocycle **IV**.[15] In contrast, reactions of *t*-BuP(NH-*t*-Bu)$_2$ with dialkylalanes R_2AlH and trialkylalanes R_3Al proceeded with elimination of only 1 equiv of dihydrogen and RH, respectively.[16] The solid-state structures of the resulting oily products could not be investigated by single-crystal X-ray diffraction. Therefore, we reinvestigated the equimolar reaction of *t*-BuP(NH-*t*-Bu)$_2$ with base-stabilized alanes $H_3Al-NMe_3$ and $H_3Al-NMe_2Et$ in order to obtain information on the solid-state structure of the first reaction product. In particular, the question of whether intra- or intermolecularly stabilized compounds of types **V** and **VI** (Chart 2) will be formed was of interest.

Both reactions in pentane at ambient temperature resulted in the elimination of 1 equiv of dihydrogen and the formation of [*t*-BuP(NH-*t*-Bu)N(*t*-Bu)$AlH_2]_2$ (**1**) in almost quantitative yield. In contrast, the reaction with

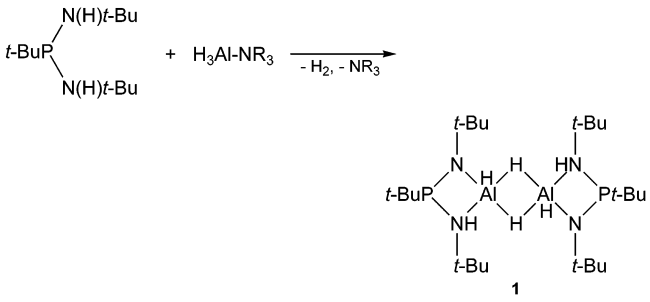

1

$H_3Al-NMe_2Et$ in refluxing toluene occurred with elimination of 2 equiv of dihydrogen and the formation of heterocyclic *t*-BuP(μ-N-*t*-Bu)$_2$AlH(NMe_2Et), as shown by its ^{31}P NMR spectrum. *t*-BuP(μ-N-*t*-Bu)$_2$AlH(NMe_2Et)

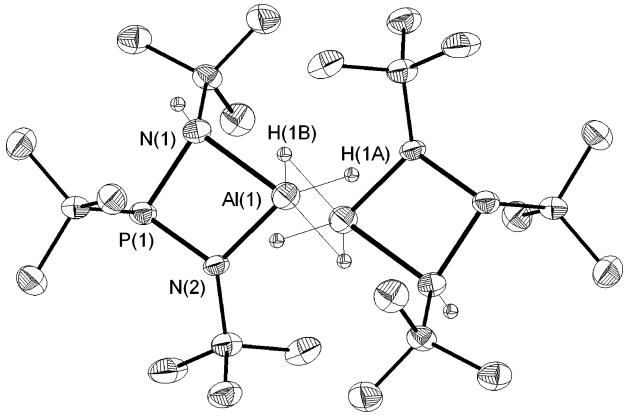

Figure 1. ORTEP diagram (50% probability ellipsoids) showing the solid-state structure and atom-numbering scheme for [*t*-BuP(NH-*t*-Bu)N(*t*-Bu)AlH_2]$_2$ (**1**). Selected bond lengths (Å) and angles (deg): P(1)−N(1) = 1.799(2), P(1)−N(2) = 1.689(2), Al(1)−N(1) = 2.094(2), Al(1)−N(2) = 1.841(2), Al(1)−H(1A) = 1.52(2), Al(1)−H(1B) = 1.66(2), Al(1)−H(1B′) = 1.88(2), P(1)−C(1) = 1.894(3), N(1)−C(5) = 1.516(3), N(2)−C(9) = 1.491(3); N(1)−P(1)−N(2) = 89.2-(2), N(1)−Al(1)−N(2) = 76.7(1), P(1)−N(1)−Al(1) = 90.5-(2), P(1)−N(2)−Al(1) = 103.5(2), C(1)−P(1)−N(1) = 99.5(2), C(1)−P(1)−N(2) = 107.6(2), C(1)−P(1)−Al(1) = 107.8(2).

has a chemical shift (121.7 ppm) similar to that of **IV** (121.2 ppm).

1 was obtained as a colorless crystalline solid in almost quantitative yield. Its ^{31}P NMR spectrum shows a singlet at 137.9 ppm, which is shifted to lower field compared to that of **IV** (121.2 ppm). The ^{1}H NMR spectrum of **1** displays singlets of the Al−H (4.81 ppm) and N−H moieties (2.16 ppm), two sets of signals for the nonequivalent *t*-BuN groups, and a doublet for the *t*-BuP moiety. No resonances due to the NMe_3 and NMe_2Et Lewis bases are observed. Signals for three chemically nonequivalent *t*-Bu groups are also detected in the ^{13}C NMR spectrum. Almost analogous NMR spectra have been previously obtained for the dialkyl- and trialkylalane reaction products,[16] which typically showed two sets of resonances for the nonequivalent *t*-BuN moieties and resonances between 135 and 140 ppm in the ^{31}P NMR spectra. The IR spectrum of **1** clearly reveals the presence of both N−H and Al−H groups due to strong absorption bands at 3291 and 1809 cm^{-1}, respectively. Its mass spectrum displays a peak with the highest mass at *m*/*z* 260, which corresponds to the monomer *t*-BuP(NH-*t*-Bu)N(*t*-Bu)AlH_2, whereas the molecular ion peak of **1** (dimer) was not detected.

Suitable crystals of **1** for a single-crystal X-ray structure determination were obtained from a solution in pentane at −30 °C. The central structural motif of **1** is two four-membered AlN_2P heterocycles which are connected by two unsymmetric Al−H−Al bridging units (Figure 1). **1** shows a crystallographic C_i symmetry, leading to structurally and chemically equivalent AlN_2P rings. The 3-fold-coordinated P atom adopts a pyramidal geometry (sum of bond angles $\sum\angle = 296.3°$). In contrast, the 3-fold-coordinated N center is almost planar ($\sum\angle = 356.4°$) and the 4-fold-coordinated center adopts a distorted-tetrahedral environment. Comparable findings were observed for *t*-BuP(μ-N-*t*-Bu)$_2$AlH(NMe_3) (**IV**), even though the N centers are both 3-fold coordinated. Repulsive interactions between the very bulky *t*-Bu and NMe_3 groups prevents them from achieving planarity ($\sum\angle = 335.7, 351.3°$).[17] In addition, the sum of the bond angles at the P atom ($\sum\angle = 300.7°$) in **IV** is also slightly larger than that in **1**, indicating stronger steric interactions between the organic substituents. This is also illustrated by the significantly enlarged C−P−Al bond angle (118.7(1)° for **IV**, 107.8(1)° for **1**). The endocyclic N(1)−P(1)−N(2) and N(1)−Al(1)−N(2) bond angles (89.2-(1), 76.7(1)°) of **1** are comparable to those of **IV**, whereas the endocyclic P(1)−N(1/2)−Al(1) angles of **1** (N(1), 90.5-(1)°; N(2), 103.5(1)°) and **IV** (N(1), 92.5(1)°; N(2), 93.1-(1)°) differ significantly due to the unequally coordinated N centers. Consequently, the P−N bond lengths of **1** (P(1)−N(2) = 1.689(2) Å, P(1)−N(1) = 1.799(2) Å) show a large variation, whereas those of **IV** are almost equidistant (173.3(1), 173.5(1) Å). This is typical for "regular" PN_2E four-membered heterocycles (E = main-group element) and has been observed in (*t*-BuN)*t*-BuP-(μ-N-*t*-Bu)$_2$B-*t*-Bu (1.710(2) Å),[18] RP(μ-N-*t*-Bu)$_2$$SiMe_2$ (1.741(3) Å),[19] and $(Me_3Si)_2NP(\mu\text{-}NR')_2Si(t\text{-}Bu)_2$ (1.769-(2) Å).[20] The dative Al−N(1) bond distance (2.094(2) Å) is about 25 pm longer than the regular Al−N(2) σ-bond (1.841(1) Å), as was expected for this bond type. These findings also correspond very well to the increased coordination number of the N(1) compared to the N(2) center (4 vs 3). The Al atom in **1** is 5-fold coordinated by two N and three H atoms. The terminal Al−H bond (1.52(2) Å) of **1** is slightly longer than that of **IV** but shorter than the bridging Al−H bonds (1.66(2), 1.88(2) Å) within the four-membered Al_2H_2 heterocycle. Analogous structural distortions have been observed for comparable intramolecular base-stabilized, 5-fold-coordinated $RAlH_2$ compounds.[21] The Al−Al distance of 2.743(2) Å is slightly longer than that observed in Al_2Me_6 (2.599 Å)[22] but agrees very well with Al−Al distances that have been previously reported for such compounds.[21]

The solid-state structure of **1** clearly reveals the principle of intramolecular stabilization to be very powerful for the generation of monosubstituted bis-(amino)phosphane fragments. Consequently, the previously described dialkyl- and trialkylalane reaction products are also expected to adopt such intramolecularly stabilized structures. Whether monomeric or dimeric units will be formed remains still unclear; however, monomeric units seem to be more likely because 5-fold-coordinated Al centers tend to occur only with small substituents such as H atoms.

To extend our investigations on the reactivity of *t*-BuP(NH-*t*-Bu)$_2$ to other group 13 element compounds, we performed reactions with less acidic boranes (H_3B−

(17) We reinvestigated the solid-state structure of **IV**, due to the high residual electron density found in the first structure analysis, and collected a much better data set, which shows only very small variations in bond lengths and distances.

(18) Gudat, D.; Niecke, E.; Nieger, M.; Paetzold, P. *Chem. Ber.* **1988**, *121*, 565.

(19) (a) Scherer, O. J.; Püttmann, M.; Krüger, C.; Wolmershäuser, G. *Chem. Ber.* **1982**, *115*, 2076. (b) Bitter, W.; Niecke, E. *Chem. Ber.* **1976**, *109*, 415. (c) Klingebiel, U. *Chem. Ber.* **1978**, *111*, 2735.

(20) Niesmann, J.; Klingebiel, U.; Rudolph, S.; Herbst-Irmer, R.; Noltemeyer, M. *J. Organomet. Chem.* **1996**, *515*, 43.

(21) See for instance: (a) Hair, G. S.; Battle, S. L.; Cowley, A. H.; Jones, R. A. *Inorg. Chem.* **2000**, *39*, 27. (b) Cui, C.; Roesky, H. W.; Noltemeyer, M.; Schmidt, H.-G. *Organometallics* **1999**, *18*, 5120. (c) Isom, H. S.; Cowley, A. H.; Decken, A.; Sissingh, F.; Corbelin, S.; Lagow, R. J. *Organometallics* **1995**, *14*, 2400. (d) Dümichen, U.; Thiele, K.-H.; Gelbrich, T.; Sieler, J. *J. Organomet. Chem.* **1995**, *495*, 71.

(22) Vranka, R. G.; Amma, E. L. *J. Am. Chem. Soc.* **1967**, *89*, 3121.

thf, H_3B-NMe_3), gallanes ($H_3Ga-NMe_3$, Me_3Ga), and indanes (Me_3In) in noncoordinating solvents (pentane, hexane). It was found that these reactions occurred with complexation of the Lewis basic P(III) center rather than with N−H activation, yielding simple Lewis acid−Lewis base adducts of the type (t-BuNH)$_2$(t-Bu)P-MR_3 (MR_3 = BH_3 (**2**), GaH_3 (**3**), $GaMe_3$ (**4**), $InMe_3$ (**5**)). These

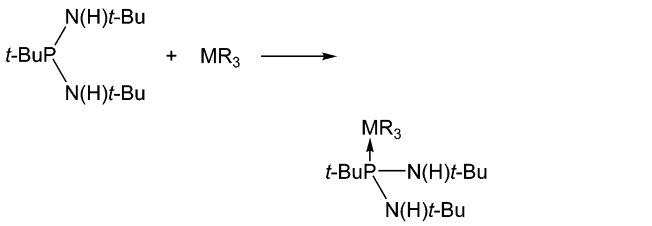

MR_3 = BH_3 **2**, GaH_3 **3**, $GaMe_3$ **4**, $InMe_3$ **5**

findings are in accordance with the expectations due to the HSAB principle. Boranes, gallanes, and indanes are soft Lewis acids which prefer coordination by the weak Lewis basic site of aminophosphanes (P center) rather than by the hard Lewis acidic N center.

2−**5** were obtained after subsequent workup as colorless solids. The ^{31}P NMR spectrum of **2** shows a quartet at 80.8 ppm with a typical $^1J_{B-P}$ coupling constant of 73.1 Hz, clearly proving the complexation of the Lewis acidic borane by the P(III) center. This is also demonstrated by its ^{11}B NMR spectrum showing a doublet at −36.1 ppm. The ^{31}P NMR spectra of **3** shows a singlet at 53.3 ppm. In contrast, **4** (51.6 ppm) and **5** (50.9 ppm) show singlets at almost the same chemical shift as t-BuP(NH-t-Bu)$_2$ (50.4 ppm). Comparable findings were observed in the ^{1}H and ^{13}C NMR spectra of **3**−**5**, showing signals due to the organic groups (t-BuP, t-BuN, NH, MR_3) at chemical shifts similar to those of the starting compounds. This indicates **3**−**5** to be extensively dissociated in solution at ambient temperature. Temperature-dependent ^{1}H and ^{31}P NMR studies between −60 and 25 °C in toluene-d_8 only showed the resonances due to the starting reagents. Peaks with the highest mass (m/z 232) observed in the mass spectra of **3**−**5** correspond to the bis(amino)phosphane t-BuP(NH-t-Bu)$_2$, indicating that the adducts are fully dissociated under these specific gas-phase conditions.

Several attempts to determine the solid-state structures of **2**−**5** by single-crystal X-ray diffraction failed, due to severe disorder problems. However, the data sets obtained from several crystals clearly proved the atom connectivity of the reaction products.[23] Finally, we succeeded in the determination of the solid-state structure of **3** (Figure 2). Suitable crystals were obtained from a solution in hexane at −30 °C. Two crystallographic independent molecules were found in the asymmetric unit. **3** is only the fifth structurally characterized phosphane−GaH_3 adduct known to date.[24] The degree of pyramidalization of the 4-fold-coordinated P atom ($\sum\angle$(N(1)−P−N(2) + C−P−N(1/2))) is significantly decreased ($\sum\angle$ = 313.3°) compared to that of **1** ($\sum\angle$ = 296.3°) and t-BuP(μ-N-t-Bu)$_2$AlH(NMe$_3$) (**IV**; $\sum\angle$ = 290.7°). This clearly is a consequence of the adduct formation, which typically leads to wider bond angles at the Lewis base.[25] The P−C bond lengths found for **3** (1.889(6)/1.854(6) Å) are comparable to those observed for **1** and **IV**, whereas the P−N bond distances (1.652(4), 1.679(4)/1.642(4), 1.655(4) Å) are significantly shorter. The Ga atoms adopt distorted-tetrahedral environments, which is typical for such Lewis acid−Lewis base adducts. The H atoms at each Ga center were localized but were fixed for the structure refinement. The P−Ga bond lengths of 2.445(2) and 2.440(2) Å agree very well with values previously reported for GaH_3−phosphane adducts. In contrast, the simple trialkylgallane adducts $R_3P-GaR'_3$ show significantly longer P−Ga bond distances (2.54−2.68 Å)[26] as a result of the decreased Lewis acidity of GaR_3 compared to GaH_3 and, more importantly, the increased steric interactions between the organic substituents. Only $Me_3P-GaMe_3$, which contains sterically less demanding methyl groups, shows a comparable P−Ga bond distance of 2.446(2) Å.[27]

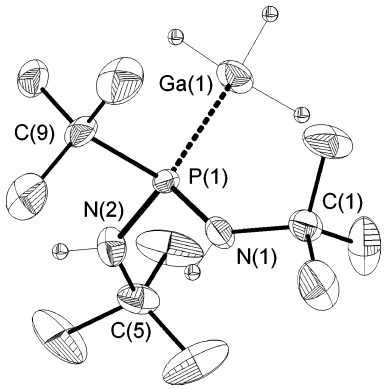

Figure 2. ORTEP diagram (50% probability ellipsoids) showing the solid-state structure and atom-numbering scheme for t-Bu(NH-t-Bu)$_2$P−GaH_3 (**3**). Only one molecule is shown for clarity. Selected bond lengths (Å) and angles (deg): P(1)−N(1) = 1.652(4), P(1)−N(2) = 1.679(4), P(1)−C(9) = 1.889(6), P(1)−Ga(1) = 2.445(2), N(1)−C(1) = 1.494(6), N(2)−C(5) = 1.505(6); N(1)−P(1)−N(2) = 108.4(2), N(1)−P(1)−C(9) = 106.5(2), N(2)−P(1)−C(9) = 99.4(2), N(1)−P(1)−Ga(1) = 117.9(2), N(2)−P(1)−Ga(1) = 114.3(2), C(9)−P(1)−Ga(1) = 108.5(2).

The complexation reactions clearly demonstrated that the N−H groups of t-BuP(NH-t-Bu)$_2$ *cannot* be activated by reactions with boranes, gallanes, and indanes but only with stronger Lewis acidic alanes. Our interest in analogous Ga- and In-containing compounds of the "alane type" prompted our interest in the synthesis of alternative starting reagents. Lithium halide elimina-

(23) Several data sets were obtained for **2**, **4**, and **5** which could not be refined due to the same disorder problem. The asymmetric unit contains two half-occupied molecules with a noncrystallographic mirror plane between and the group 13 atom (B, **2**; Ga, **4**; In, **5**) and one C atom of the t-BuP group on the plane (occupancy 1). However, the connectivity of all compounds (P coordination!) was confirmed without any doubts.

(24) (a) O'Hare, D. O.; Foord, J. S.; Page, T. C. M.; Whitaker, T. J. *J. Chem. Soc., Chem. Commun*. **1991**, 1445. (b) Atwood, J. L.; Robinson, K. D.; Bennett, F. R.; Elms, F. M.; Koutsantonis, G. A.; Raston, C. L.; Young, D. J. *Inorg. Chem*. **1992**, *31*, 2673. (c) Elms, F. M.; Gardiner, M. G.; Koutsantonis, G. A.; Raston, C. L.; Atwood, J. L.; Robinson, K. D. *J. Organomet. Chem*. **1993**, *449*, 45.

(25) The structural changes according to the adduct formation have been described by Haaland in detail. Haaland, A. In *Coordination Chemistry of Aluminum*; Robinson, G. H., Ed.; VCH: Weinheim, Germany, 1993.

(26) See for instance: (a) Wells, R. L.; Baldwin, R. A.; White, P. S. *Organometallics* **1995**, *14*, 2123. (b) Wells, R. L.; Aubuchon, S. R.; Self, M. F.; Jasinski, J. P.; Woudenberg, R. C.; Butcher, R. J. *Organometallics* **1992**, *11*, 3370. (c) Banks, M. A.; Beachley, O. T., Jr.; Maloney, J. D.; Rogers, R. D. *Polyhedron* **1990**, *9*, 335.

(27) Burns, J. A.; Pennington, W. T.; Robinson, G. H. *Organometallics* **1995**, *14*, 1533.

tion reactions have been proven in the past to be very powerful for the generation of compounds containing Ga−N and In−N bonds. Consequently, we investigated deprotonation reactions of *t*-BuP(NH-*t*-Bu)$_2$ using *n*-BuLi in attempt to synthesize the corresponding mono- and dilithiated reaction products. Nöth et al. recently reported on the synthesis and solid-state structures of several dilithiated bis(amido)phosphanes.[10a]

The reaction between equimolar amounts of *n*-BuLi and *t*-BuP(NH-*t*-Bu)$_2$ in Et$_2$O at −78 °C, followed by slow warming to ambient temperature, occurred with smooth gas evolution. **6** was obtained in almost quantitative yield as a colorless crystalline solid.

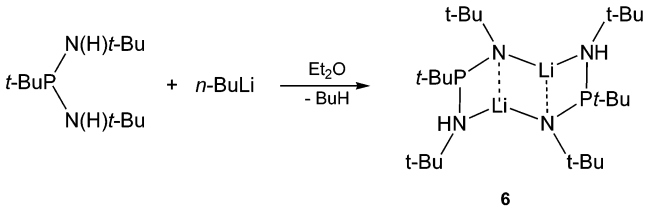

6

The ^{31}P NMR spectra of **6** in noncoordinating solvents such as hexane and C_6D_6 only show a singlet at 103.9 ppm, which is shifted downfield compared to that of the protonated bis(amino)phosphane *t*-BuP(N(H)*t*-Bu)$_2$. In contrast, the ^{31}P NMR spectra of both isolated and in situ prepared **6** in Et$_2$O show an additional signal of lower intensity (about 10%) at 108 ppm. Obviously, coordinating solvents such as Et$_2$O are able to transform **6** into its solvent-coordinated form, with both forms forming an equilibrium in solution. Unfortunately, the Et$_2$O-coordinated form could not be isolated. The Et$_2$O molecule(s) were found to be only weakly bonded and were removed under typical vacuum conditions during workup, as was demonstrated by NMR spectroscopy. Both the ^{1}H and ^{13}C NMR spectra of **6** only show signals due to the organic groups of the bis(amino)phosphane moiety (*t*-BuP, *t*-BuN, NH), whereas no resonances due to the presence of Et$_2$O were detected. The mass spectrum of **6** shows a peak with the highest mass at *m*/*z* 232, which corresponds to the bis(amino)phosphane *t*-BuP(NH-*t*-Bu)$_2$, due to decomposition of **6** under these conditions.

The solid-state structure of **6** was determined by single-crystal X-ray analysis (Figure 3). Suitable crystals were obtained from a solution in Et$_2$O at −30 °C. The central structural motif of **6** is a nonplanar eight-membered $P_2N_4Li_2$ heterocycle consisting of two (anionic) bis(amino)phosphane moieties and two Li cations. Very recently, we described the reaction of *t*-BuP(NH$_2$)$_2$ and Et$_2$AlH, yielding the first alumonitridophosphinate, [*t*-BuP(H)(NH)$_2$AlEt$_2$]$_2$ (**III**). The central structural motif of **III** was also an eight-membered heterocycle. In contrast to **III**, **6** has a 3-fold-coordinated P(III) atom and contains two sets of nonequivalent N atoms (two *t*-BuN and two *t*-Bu(H)N units). Both Li cations are coordinated by three N atoms with two short N−Li contacts (N(1)−Li(1) = 1.997(4) Å, N(2)−Li(1) = 2.030(4) Å) and one long N−Li bond length (N(3)−Li(1) = 2.098(4) Å). In addition, one Li···Li (Li(1)−Li(2) = 2.296(5) Å) and two short Li···H contacts (H(7A)−Li(1) = 2.23 Å, H(7C)−Li(1) = 2.42 Å/H(19B)−Li(2) = 2.35 Å, H(19A)−Li(2) = 2.34 Å) result in a distorted-octahedral coordination for each Li cation. Three additional Li···H

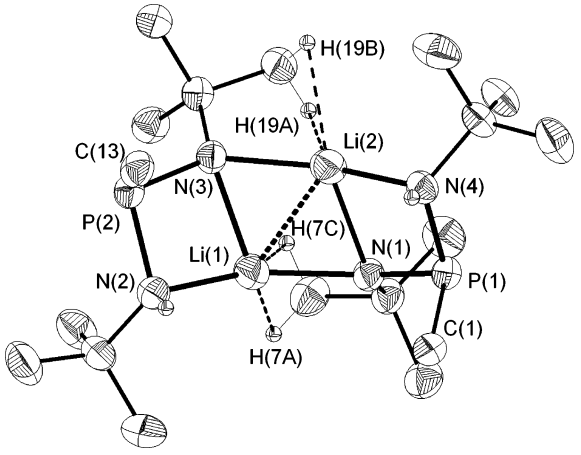

Figure 3. ORTEP diagram (50% probability ellipsoids) showing the solid-state structure and atom-numbering scheme for [*t*-BuP(NH-*t*-Bu)N(*t*-Bu)Li]$_2$ (**6**). Only the α-C atom of each *t*-Bu-P group is shown for clarity. Selected bond lengths (Å) and angles (deg): P(1)−N(1) = 1.675(2), P(1)−N(4) = 1.778(2), P(1)−C(1) = 1.900(2), P(2)−N(2) = 1.776(2), P(2)−N(3) = 1.677(2), P(2)−C(1) = 1.893(2), Li(1)−N(1) = 1.997(4), Li(1)−N(2) = 2.030(4), Li(1)−N(3) = 2.098(4), Li(2)−N(1) = 2.096(4), Li(2)−N(3) = 2.012(4), Li(2)−N(4) = 2.041(4), Li(1)−Li(2) = 2.296(5), Li(1)−H(7A) = 2.23, Li(1)−H(7C) = 2.42, Li(2)−H(19B) = 2.35, Li(2)−H(19A) = 2.34; N(1)−P(1)−N(4) = 98.8(1), N(3)−P(2)−N(2) = 98.8(1), N(1)−Li(1)−N(2) = 148.3(2), N(1)−Li(1)−N(3) = 111.0(2), N(2)−Li(1)−N(3) = 78.9(2), N(3)−Li(2)−N(4) = 149.3(2), N(3)−Li(2)−N(1) = 110.6(2), N(4)−Li(2)−N(1) = 78.7(2), Li(1)−N(1)−Li(2) = 68.2(2), Li(2)−N(3)−Li(1) = 67.9(2).

distances (H(10A)−Li(1) = 2.73 Å, H(12B)−Li(1) = 2.78 Å, H(2A)−Li(1) = 2.82 Å/H(16A)−Li(2) = 2.78 Å, H(22C)−Li(2) = 2.60 Å, H(24B)−Li(2) 2.79 Å) were found for both Li cations but were not stereochemically considered because their contribution in stabilizing the Li cation is expected to be quite low. The bonding parameters for the second Li atom (Li(2)) are almost the same and will therefore not be discussed in detail here. The relatively long P(1)−C(1) bond (1.900(2) Å) and the sum of the bond angles of the P(1) atom ($\sum\angle$ = 305.7°) of **6** are comparable to those found in **1** and **IV**. The N centers in **6** are nonequivalent because of their different coordination numbers. This is clearly reflected by the different Li−N and P−N bond distances (P(1)−N(4) = 1.778(2) Å, P(1)−N(1) = 1.675(2) Å) within each four-membered PN_2Li ring. Comparable findings were observed for **1**. To our surprise, the endocyclic P−N−Li bond angles in **6** (P(1)−N(1)−Li(2) = 91.6(2)°, P(1)−N(4)−Li(2) = 90.5(2)°, P(2)−N(2)−Li(1) = 90.5(2)°, P(2)−N(3)−Li(1) = 91.0(2)°) are almost equal, as was observed for **IV** (P(1)−N(1/2)−Al(1) = 92.5(1), 93.1(1)°), whereas **1** shows significantly different endocyclic P(1)−N(1/2)−Al(1) bond angles of 90.5(1) and 103.5(1)°, respectively. The endocyclic Li−N−Li bond angles (67.9(2), 68.2(2)°) of the four-membered N_2Li_2 ring are significantly smaller than the N−Li−N bond angles (110.6(2), 111.0(2)°) due to the increased Lewis acidity of N compared to Li.

As mentioned earlier, **6** forms an equilibrium with its solvent-coordinated form in coordinating solvents such as Et$_2$O and THF. However, the Lewis basicity of Et$_2$O and THF was too low to prevent the reaction product from dimerization. Consequently, the question arose if

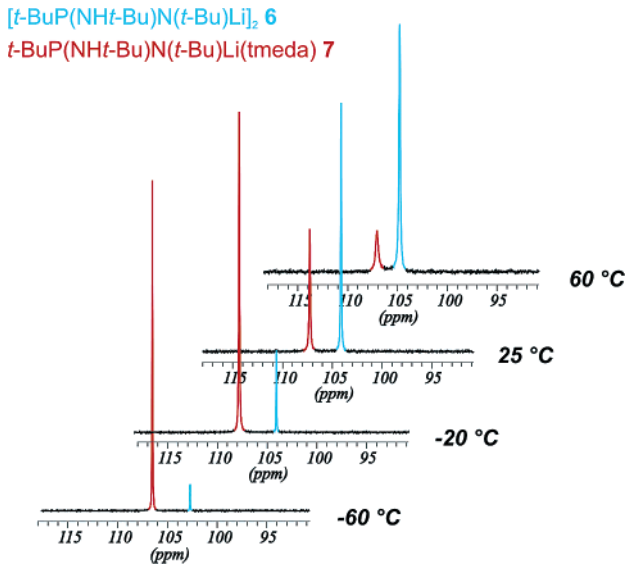

Figure 4. Temperature-dependent ^{31}P NMR study of **7** in toluene-d_8.

it might be possible to obtain a monomeric amidophosphane by reaction with a stronger Lewis base. Dissolving **6** in tetramethylenediamine (tmeda) as well as the deprotonation reaction of *t*-BuP(NH-*t*-Bu)$_2$ with *n*-BuLi in tmeda yielded the monomer **7** in high yield.

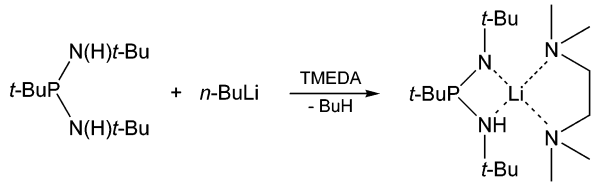

7

A solution of isolated **7** in tmeda as well as of in situ prepared **7** shows *one* ^{31}P resonance (108 ppm), which is shifted slightly downfield compared to that of **6**. In contrast, the ^{31}P NMR spectrum of **7** dissolved in C_6D_6 shows *two* ^{31}P resonances (104.2, 107,4 ppm). These findings point to the formation of an equilibrium between tmeda-coordinated **7** and unsolvated **6** in noncoordinating solvents. Consequently, two sets of signals were also observed in the ^{1}H and ^{13}C NMR spectra of **7**, with one set of resonances corresponding to those observed for **6**. Two additional peaks (2.07, 2.23 ppm) clearly demonstrate the presence of one tmeda molecule. The equilibrium is strongly temperature dependent, as was demonstrated by NMR spectroscopy. At −60 °C, the ^{31}P NMR spectrum of **7** (toluene-d_8) shows a major resonance at 105.4 ppm, which can be assigned to the tmeda complex **7**, and a second resonance in very low intensity (6%) at 101.6 ppm, which corresponds to the unsolvated dimer **6**. Raising the temperature shifts the equilibrium toward **6**. At +60 °C the major peak corresponds to **6** (relative intensity 74% (**6**), 26% (**7**)). Figure 4 displays the temperature-dependent ^{31}P NMR spectra.

The purity of **7** was proven by powder X-ray diffraction. The experimentally observed diffraction pattern of **7** agrees very well with the pattern calculated from the single-crystal X-ray data of **7** (Figure 5[28]). No further reflections which indicate the presence of **6** were detected (see the Supporting Information).

Crystals of **7** suitable for a single-crystal X-ray structure analysis were obtained from a solution in tmeda at −30 °C. **7** forms a four-membered PN_2Li heterocycle in the solid state which is stabilized by one tmeda molecule (Figure 6).

The N−Li bond distances within the PN_2Li ring differ significantly (N(2)−Li(1) = 1.976(3) Å, N(1)−Li(1) = 2.161(3) Å), as was expected due to the presence of two differently coordinated N atoms (*c.n.* 3 N(2), 4 N(1)). The tmeda molecule does not coordinate in a symmetrical fashion to the Li cation, as is clearly reflected by the N−Li bond distances. These differ by almost 20 pm (N(4)−Li(1) = 2.130(3) Å, N(3)−Li(1) = 2.323(3) Å), most likely due to steric interactions. The endocyclic N(3)−Li(1)−N(4) bond angle is 83.1(1)°. Two very long Li···H contacts (H(12A)−Li(1) = 2.86 Å, H(6A)−Li(1) = 2.83 Å) indicate some additional weak interaction, but their stabilizing effect is expected to be rather low.[29] Consequently, the coordination environment of the Li cation should be described as distorted tetrahedral. As was observed in **6**, **7** contains a 3-fold-coordinated P atom ($\sum\angle$ = 303.1°). The endocyclic N(1)−P(1)−N(2) bond angle (98.3(1)°) is comparable to that found in **6** (98.8(9)°). In contrast, the presence of the Al centers in the four-membered rings of **1** and **IV** significantly decrease the endocyclic N−P−N bond angles (89.7(1)°, **IV**; 89.2(2)°, **1**). This is most likely a structural consequence of the longer Li−N distance compared to the (stronger) Al−N bond distances. Comparable trends were observed for the endocyclic N−Al−N bond angles in **IV** (83.4(1)°) and in **1** (76.7(1)°) as well as the N−Li−N bond angles in **6** (77.9(2), 78.7(2)°) and in **7** (77.8(1)°). These show a maximum widening in **IV** due to the formation of two regular Al−N σ-bonds. The P−N bond distances in **7** also differ by almost 13 pm (P(1)−N(1) = 1.784(2) Å, P(1)−N(2) = 1.654(2) Å), as was found in **1** and **6**.

Initial studies on the general reactivity of **6** were performed with an in situ prepared sample. The reaction with an equimolar amount of $GaCl_3$ in Et_2O occurred with elimination of LiCl, leading to the formation of *t*-BuP(NH-*t*-Bu)N(*t*-Bu)$GaCl_2$ (**8**).

$$\mathbf{6} + GaCl_3 \xrightarrow[-LiCl]{+Et_2O} \underset{\mathbf{8}}{t\text{-BuP(NH-}t\text{-Bu)N(}t\text{-Bu)GaCl}_2}$$

8 was obtained as a colorless crystalline solid in almost quantitative yield. Its ^{31}P NMR spectrum shows a singlet at 137.7 ppm, comparable to that obtained for the aluminum derivatives *t*-BuP(NH-*t*-Bu)N(*t*-Bu)AlR_2 (R = H (**1**), Me, Et, *i*-Bu[16]). As was observed in **1**, the ^{1}H NMR spectrum of **8** displays singlets of the N−H group (3.12 ppm), two sets of signals for the *t*-BuN groups, and a doublet for the *t*-BuP moiety. Signals for three different *t*-Bu groups were also detected in the ^{13}C NMR spectrum. The IR spectrum of **8** displays a strong absorption band of the N−H group at 3239 cm^{-1}.

(28) The theoretical pattern was calculated[36] using the room-temperature lattice parameters (see the Experimental Section), and the atomic parameters were obtained by a single-crystal structure analysis (data set taken at 123(2) K; see Table 1 in the Supporting Information).

(29) However, these distances are shorter than the rest of the Li···H distances, which are longer than 3.0 Å.

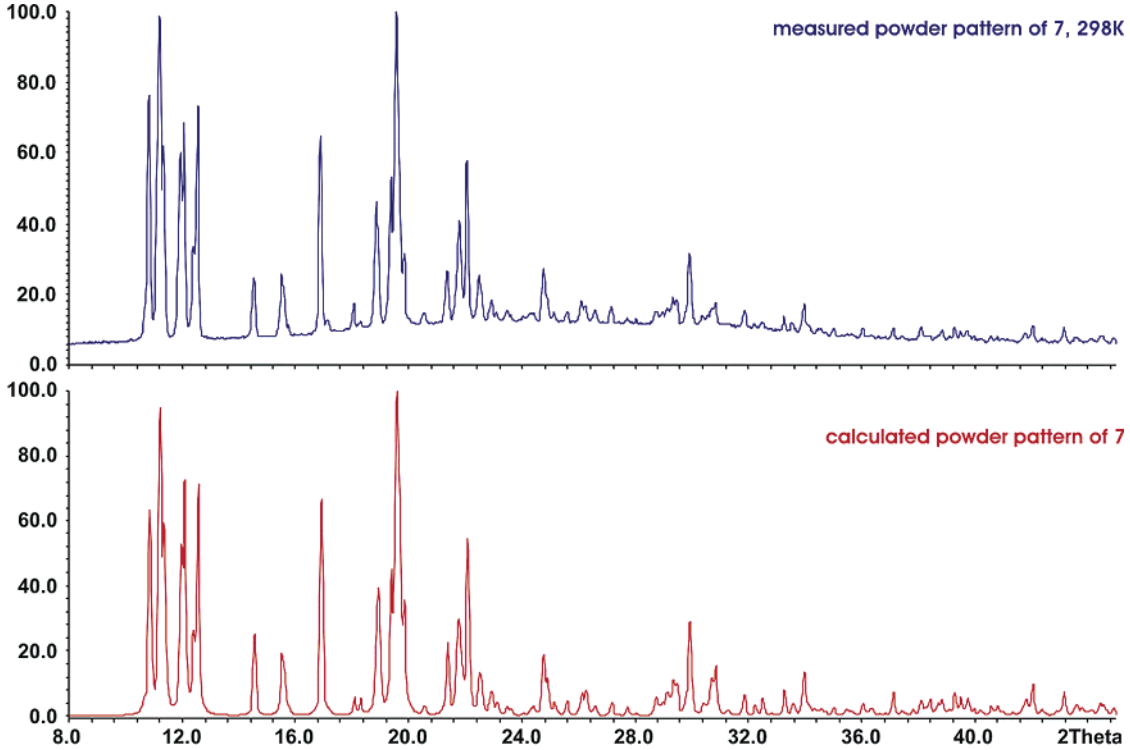

Figure 5. Experimental and calculated powder X-ray diffraction pattern of **7**.

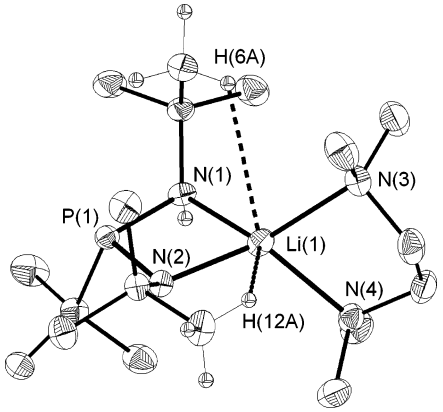

Figure 6. ORTEP diagram (50% probability ellipsoids) showing the solid-state structure and atom-numbering scheme for *t*-BuP(NH-*t*-Bu)N(*t*-Bu)Li(tmeda) (**7**). Selected bond lengths (Å) and angles (deg): P(1)−N(1) = 1.784(2), P(1)−N(2) = 1.654(2), P(1)−C(1) = 1.905(2), Li(1)−N(1) = 2.161(3), Li(1)−N(2) = 1.976(3), Li(1)−N(3) = 2.323(3), Li(1)−N(4) = 2.130(3), Li(1)−H(12A) = 2.86, Li(1)−H(6A) = 2.83, Li(1)−H(4) = 1.972(5); N(1)−P(1)−N(2) = 98.3(1), N(1)−Li(1)−N(2) = 77.8(2), N(3)−Li(1)−N(4) = 83.1(2), P(1)−N(1)−Li(1) = 86.8(1), P(1)−N(2)−Li(1) = 96.8(2), N(1)−P(1)−C(1) = 98.3(1), N(2)−P(1)−C(1) = 106.6(1), C(1)−P(1)−Li(1) = 113.0(1).

Unfortunately, single crystals of **8** could not be obtained, allowing no further discussion of its solid-state structure.

Conclusions

Reactions of the bis(amino)phosphane *t*-BuP(NH-*t*-Bu)$_2$ with group 13 trihydrides and trialkyls as well as *n*-BuLi were investigated in detail. It was demonstrated that alanes react at the N−H group with formation of aminoalanes, whereas boranes, gallanes, and indanes MR_3 (R = H, Me) prefer Lewis acid−Lewis base adduct formation at the P center. In contrast, solvated or unsolvated Li amidophosphanes, which can be obtained by reaction with an equimolar amount of *n*-BuLi, react with $GaCl_3$ to give the N-functionalized compound. The solid-state structure of the Li amidophosphane strongly depends on the nature of the solvent. Strong Lewis basic, chelating solvents such as tmeda yield solvated monomeric compounds, whereas an unsolvated dimer is formed in Et_2O. The reactivity of such monolithiated compounds toward chloro- and bromogallanes and chloro- and bromoindanes RMX_2 and R_2MX as well as the synthesis of dilithiated compounds is currently under investigation. In addition, the potential of as-prepared group 13 derivatives with respect to their application as *single-source precursors* for the deposition of the corresponding material films by use of MOCVD processes will be studied in detail.

Experimental Section

General Considerations. All manipulations were performed in a glovebox under an Ar atmosphere or by standard Schlenk techniques. *t*-BuP(NH-*t*-Bu)$_2$,[16] $H_3Al{-}NMe_3$,[30] $H_3Al{-}N(Et)Me_2$,[30] $H_3Ga{-}NMe_3$,[31] Me_3Ga,[32] and Me_3In[33] were prepared according to literature methods, whereas H_3B(thf), $GaCl_3$, and *n*-BuLi were commercially available from Aldrich and were used as received. ^{1}H, ^{13}C{^{1}H}, ^{31}P{^{1}H}, ^{11}B{^{1}H}, and ^{7}Li{^{1}H} spectra were recorded using a Bruker AMX 300 spectrometer and are referenced to internal C_6D_5H (δ(^{1}H) 7.154, δ(^{13}C) 128.0) and external H_3PO_4 (85%, ^{31}P), $BF_3(OEt_2)$ (^{11}B), and LiCl (9.7 M in D_2O, ^{7}Li). Low-temperature NMR

(30) Brauer, G. In *Handbuch der präparativen Anorganischen Chemie*; Ferdinand Enke Verlag: Stuttgart, Germany, 1975; p 823.
(31) Shriver, D. F.; Shirk, A. E. *Inorg. Synth.* **1977**, *17*, 42.
(32) Foster, D. F.; Cole-Hamilton, D. J.; Jones, R. A. *Inorg. Synth.* **1997**, *31*, 46.
(33) Foster, D. F.; Cole-Hamilton, D. J.; Jones, R. A. *Inorg. Synth.* **1997**, *31*, 33.

spectra are referenced to internal toluene-d_8 (δ(^{1}H) 7.20). Melting points were measured in sealed capillaries and are not corrected. Elemental analyses were performed at the Mikroanalytisches Labor der Universität Bonn.

[*t*-BuP(NH-*t*-Bu)N(*t*-Bu)AlH$_2$]$_2$ (1). A solution of *t*-BuP(NH-*t*-Bu)$_2$ (1 mmol) in pentane (30 mL) was combined at −70 °C with an equimolar amount of H$_3$Al−NMe$_3$ (1 mmol), which was dissolved in pentane (20 mL). The solution was slowly warmed to ambient temperature, leading to a smooth gas evolution, and stirred for an additional 1 h. Storage at −30 °C yielded colorless crystals, which were isolated by filtration.

Yield: 1.30 g (83%). Mp: 125 °C. Anal. Found (calcd) for $C_{24}H_{60}Al_2N_4P_2$ (M_r = 520.67): C, 54.73 (55.20); H, 11.51 (11.52). ^{1}H NMR (300 MHz, C_6D_6, 25 °C): δ 1.00 (d, $^3J_{P-H}$ = 11.9 Hz, 18H, PC*Me*$_3$), 1.14 (s, 18H, NC*Me*$_3$), 1.37 (d, $^4J_{P-H}$ = 1.0 Hz, 18H, N(H)C*Me*$_3$), 2.16 (m, br, 2H, N*H*), 4.81 (s, br, 4H, AlH). ^{13}C{^{1}H} NMR (74 MHz, C_6D_6, 25 °C): δ 25.8 (d, $^2J_{P-C}$ = 17.8 Hz, PC*Me*$_3$), 28.4 (d, $^3J_{P-C}$ = 7.1 Hz, N(H)C*Me*$_3$), 33.6 (d, $^3J_{P-C}$ = 8.4 Hz, NC*Me*$_3$), 34.6 (d, $^1J_{P-C}$ = 33.3 Hz, P*C*Me$_3$), 51.5 (d, $^2J_{P-C}$ = 17.8 Hz, N*C*Me$_3$), 54.3 (d, $^2J_{P-C}$ = 12.6 Hz, N(H)-*C*Me$_3$). ^{31}P{^{1}H} NMR (121 MHz, C_6D_6, 25 °C): δ 137.9 (s). EI-MS (12 eV, 150 °C; *m*/*z* (%)): 260 (10) [M/2]$^+$, 203 (100) [M − Al(H)$_2$N(*t*-Bu)P(*t*-Bu)N(H)*t*-Bu − *t*-Bu]$^+$, 175 (48) [M − Al(H)$_2$N(*t*-Bu)P(*t*-Bu)N(H)*t*-Bu − *t*-Bu − AlH]$^+$, 145 (68) [M − Al(H)$_2$N(*t*-Bu)P(*t*-Bu)N(H)*t*-Bu − 2 *t*-Bu − H]$^+$, 102 (25) [*t*-BuPN]$^+$, 57 (48) [*t*-Bu]$^+$. IR (film, KBr plates): ν 3291 (N−H), 1809 (Al−H), 1210, 1198, 1026, 833 cm^{-1}.

***t*-Bu(NH-*t*-Bu)$_2$P−BH$_3$ (2).** A 3 mL portion of H$_3$B−thf (1 M in THF, 3 mmol) was added at ambient temperature via syringe to a solution of *t*-BuP(NH-*t*-Bu)$_2$ (0.70 g, 3 mmol) in hexane (30 mL). The resulting clear solution was stirred for 1 h and stored at 2 °C. After 72 h, colorless crystals were formed, which were isolated by filtration.

Yield: 0.70 g (95%). Mp: 149 °C. Anal. Found (calcd) for $C_{12}H_{32}BN_2P$ (M_r = 246.18): C, 57.93 (58.54); H, 12.99 (13.10). ^{1}H NMR (300 MHz, C_6D_6, 25 °C): δ 1.02 (d, $^3J_{P-H}$ = 13.8 Hz, 9H, PC*Me*$_3$), 1.25 (d, $^4J_{P-H}$ = 0.5 Hz, 18H, NC*Me*$_3$), 1.43 (m, br, 2H, N*H*), 1.52 (q, br, $^1J_{B-H}$ = 94.7 Hz, 3H, B*H*). ^{13}C{^{1}H} NMR (74 MHz, C_6D_6, 25 °C): δ 25.2 (d, $^2J_{P-C}$ = 2.9 Hz, PC*Me*$_3$), 32.5 (d, $^3J_{P-C}$ = 2.9 Hz, PNC*Me*$_3$), 32.9 (d, $^1J_{P-C}$ = 51.4 Hz, P*C*Me$_3$), 52.4 (d, $^2J_{P-C}$ = 1.3 Hz, PN*C*Me$_3$). ^{31}P{^{1}H} NMR (121 MHz, C_6D_6, 25 °C): δ 80.8 (q, $^1J_{P-B}$ = 73.1 Hz). ^{11}B{^{1}H} NMR (96 MHz, C_6D_6, 25 °C): δ −36.1 (d, $^2J_{B-P}$ = 73.1 Hz). EI-MS (12 eV, 50 °C; *m*/*z* (%)): 232 (21) [M − BH$_3$]$^+$, 175 (100) [M − BH$_3$ − *t*-Bu]$^+$, 119 (14) [M − BH$_3$ − 2 *t*-Bu]$^+$, 63 (20) [M − BH$_3$ − 3 *t*-Bu]$^+$. IR (film, KBr plates): ν 3341 (N−H), 2388, 2365, 2293 (B−H), 1234, 1201, 1006, 810, 724 cm^{-1}.

***t*-Bu(NH-*t*-Bu)$_2$P−GaH$_3$ (3).** A solution of *t*-BuP(NH-*t*-Bu)$_2$ (0.46 g, 2 mmol) in hexane (20 mL) was combined with an equimolar amount of H$_3$Ga−NMe$_3$ (0.26 g, 2 mmol) dissolved in hexane (20 mL) at −78 °C and warmed to ambient temperature within 1 h. After the mixture was stirred for 20 min, the resulting clear solution was stored at −30 °C. After 14 h, colorless crystals were formed, which were isolated by filtration.

Yield: 0.60 g (98%). Mp: 120 °C dec. Anal. Found (calcd) $C_{12}H_{32}GaN_2P$ (M_r = 305.09): C, 46.18 (47.24); H, 9.94 (10.57). ^{1}H NMR (300 MHz, C_6D_6, 25 °C): δ 0.97 (d, $^3J_{P-H}$ = 12.8 Hz, 9H, PC*Me*$_3$), 1.20 (d, $^4J_{P-H}$ = 0.7 Hz, 18H, NC*Me*$_3$), 1.36 (s, br, 2H, N*H*), 4.63 (s, br, 3H, *H*$_3$Ga). ^{13}C{^{1}H} NMR (74 MHz, C_6D_6, 25 °C): δ 25.6 (d, $^2J_{P-C}$ = 13.9 Hz, PC*Me*$_3$), 31.8 (d, $^1J_{P-C}$ = 10.7 Hz, P*C*Me$_3$), 32.9 (d, $^3J_{P-C}$ = 7.1 Hz, NC*Me*$_3$), 51.1 (d, $^2J_{P-C}$ = 12.0 Hz, N*C*Me$_3$). ^{31}P{^{1}H} NMR (121 MHz, C_6D_6, 25 °C): δ 53.3 (s). IR (film, KBr plates): ν 3318 (N−H), 1819, 1799, 1765 (Ga−H), 1227, 929, 867 cm^{-1}.

MMe$_3$ Adducts. Pure *t*-BuP(NH-*t*-Bu)$_2$ (0.46 g, 2 mmol) was combined in the glovebox with an equimolar amount of Me$_3$M, immediately forming a white solid. The products **4**−**6** were recrystallized from pentane (10 mL) at −30 °C.

***t*-Bu(NH-*t*-Bu)$_2$P−GaMe$_3$ (4).** Yield: 0.67 g (96%). Mp: 44 °C. Anal. Found (calcd) $C_{15}H_{38}GaN_2P$ (M_r = 347.17): C, 51.13 (51.90); H, 10.51 (11.03). ^{1}H NMR (300 MHz, C_6D_6, 25 °C): δ −0.09 (s, 9H, Ga*Me*$_3$), 0.96 (d, $^3J_{P-H}$ = 12.9 Hz, 9H, PC*Me*$_3$), 1.20 (d, $^4J_{P-H}$ = 0.6 Hz, 18H, NC*Me*$_3$), 1.32 (m, br, 2H, NH). ^{13}C{^{1}H} NMR (74 MHz, C_6D_6, 25 °C): δ 0.8 (s, br, *Me*$_3$Ga), 25.8 (d, $^2J_{P-C}$ = 15.5 Hz, *Me*$_3$CP), 31.6 (d, $^1J_{P-C}$ = 5.5 Hz, Me$_3$*C*P), 32.9 (d, $^3J_{P-C}$ = 7.8 Hz, *Me*$_3$CN), 50.8 (d, $^2J_{P-C}$ = 13.9 Hz, Me$_3$*C*N). ^{31}P{^{1}H} NMR (121 MHz, C_6D_6, 25 °C): δ 51.6 (s).

***t*-Bu(NH-*t*-Bu)$_2$P−InMe$_3$ (5).** Yield: 0.69 g (88%). Mp: 65 °C. Anal. Found (calcd) $C_{15}H_{38}InN_2P$ (M_r = 392.27): C, 45.21 (45.93); H, 9.53 (9.76). ^{1}H NMR (300 MHz, C_6D_6, 25 °C): δ −0.10 (s, 9H, *Me*$_3$In), 0.95 (d, $^3J_{P-H}$ = 13.1 Hz, 9H, PC*Me*$_3$), 1.19 (d, $^4J_{P-H}$ = 0.7 Hz, 18H, NC*Me*$_3$), 1.29 (m, br, 2H, N*H*). ^{13}C{^{1}H} NMR (74 MHz, C_6D_6, 25 °C): δ −1.3 (br, *Me*$_3$In), 25.7 (d, $^2J_{P-C}$ = 13.9 Hz, PC*Me*$_3$), 32.0 (d, $^1J_{P-C}$ = 7.4 Hz, P*C*Me$_3$), 32.9 (d, $^3J_{P-C}$ = 7.4 Hz, NC*Me*$_3$), 50.8 (d, $^2J_{P-C}$ = 12.6 Hz, N*C*Me$_3$). ^{31}P{^{1}H} NMR (121 MHz, C_6D_6, 25 °C): δ 50.9 (s).

[*t*-BuP(NH*t*-Bu)N(*t*-Bu)Li]$_2$ (6). *n*-BuLi (1.6 M in hexane, 2 mmol, 1.25 mL) was added dropwise to a solution of *t*-BuP(NH-*t*-Bu)$_2$ (2 mmol, 0.46 g) in Et$_2$O (20 mL) at −60 °C. The resulting clear solution was slowly warmed to ambient temperature, accompanied by a smooth gas evolution. After it was stirred for an additional 30 min, the clear solution was cooled to −30 °C. After 24 h **6** was obtained in the form of yellow crystals.

Yield: 0.43 g (90%). Mp: 100 °C. Anal. Found (calcd) $C_{24}H_{56}Li_2N_4P_2$ (M_r = 476.56): C, 58.98 (60.49); H, 11.07 (11.84). ^{1}H NMR (300 MHz, C_6D_6, 25 °C): δ 1.07 (d, $^3J_{P-H}$ = 10.9 Hz, 18H, PC*Me*$_3$), 1.18 (s, 18H, NC*Me*$_3$), 1.47 (s, 18H, N(H)C*Me*$_3$). ^{13}C{^{1}H} NMR (74 MHz, C_6D_6, 25 °C): δ 27.9 (d, $^2J_{P-C}$ = 17.5 Hz, PC*Me*$_3$), 31.9 (d, $^3J_{P-C}$ = 7.8 Hz, PN(H)C*Me*$_3$), 32.0 (d, $^1J_{P-C}$ = 32.0 Hz, P*C*Me$_3$), 35.8 (d, $^3J_{P-C}$ = 12.3 Hz, PNC*Me*$_3$), 51.7 (d, $^2J_{P-C}$ = 18.8 Hz, N*C*Me$_3$), 53.5 (d, $^2J_{P-C}$ = 31.4 Hz, N(H)*C*Me$_3$). ^{31}P{^{1}H} NMR (121 MHz, C_6D_6, 25 °C): δ 103.9 (s). ^{31}P{^{1}H} NMR (121 MHz, Et$_2$O, 25 °C, in situ spectrum): δ 105.2 (s), 108.7 (s, br). ^{7}Li{^{1}H} NMR (116 MHz, C_6D_6, 25 °C): δ 3.0 ppm (s, br). IR (film, KBr plates): ν 3320 (N−H), 1209, 1177, 1024, 969, 825, 788, 732 cm^{-1}.

***t*-BuP(NH-*t*-Bu)N(*t*-Bu)Li(tmeda) (7). 6** (0.5 mmol, 0.24 g) was dissolved in tmeda (5 mL) and stored at −30 °C. After 24 h colorless crystals of **7** were obtained. Yield: 0.34 g (96%). Alternatively, **7** was obtained by deprotonation of *t*-BuP(NH-*t*-Bu)$_2$ (2 mmol, 0.46 g) with *n*-BuLi (1.6 M in hexane, 2 mmol, 1.25 mL) in tmeda (20 mL) at −20 °C followed by warming to ambient temperature and storage at −30 °C for 24 h. Yield: 0.64 g (90%).

Mp: 64 °C. Anal. Found (calcd) for $C_{18}H_{44}LiN_4P$ (M_r = 354.48): C, 60.33 (60.99); H, 12.39 (12.51). NMR spectra obtained from C_6D_6 (^{1}H, ^{7}Li, ^{13}C, ^{31}P) show a mixture of **6** and **7** in a relative intensity of 70% (**6**) to 30% (**7**). ^{1}H NMR (300 MHz, C_6D_6, 25 °C): δ 1.07 (d, $^3J_{P-H}$ = 10.7 Hz, 18H, PC*Me*$_3$, **6**), 1.18 (s, 18H, NC*Me*$_3$, **6**), 1.21 (d, $^3J_{P-H}$ = 10.3 Hz, 9H, PC*Me*$_3$, **7**), 1.26 (s, 9H, NC*Me*$_3$, **7**), 1.47 (s, 18H, N(H)C*Me*$_3$, **6**), 1.56 (s, 9H, N(H)C*Me*$_3$, **7**), 2.07 (s, 12H, tmeda), 2.23 (s, 4H, tmeda, br). ^{13}C{^{1}H} NMR (74 MHz, C_6D_6, 25 °C): δ 27.3 (d, $^2J_{P-C}$ = 17.5 Hz, PC*Me*$_3$, **7**), 28.0 (d, $^2J_{P-C}$ = 17.5 Hz, PC*Me*$_3$, **6**), 31.9 (d, $^3J_{P-C}$ = 8.4 Hz, PN(H)C*Me*$_3$, **6**), 32.2 (d, $^3J_{P-C}$ = 9.1 Hz, PN(H)C*Me*$_3$, **7**), 35.8 (d, $^3J_{P-C}$ = 12.3 Hz, PNC*Me*$_3$, **6**), 37.5 (d, $^3J_{P-C}$ = 11.6 Hz, PNC*Me*$_3$, **7**), 46.1 (s, (tmeda-N*Me*$_2$), 51.0 (d, $^2J_{P-C}$ = 16.8 Hz, N*C*Me$_3$, **7**), 51.8 (d, $^2J_{P-C}$ = 18.8 Hz, N*C*Me$_3$, **6**), 52.2 (d, $^2J_{P-C}$ = 28.5 Hz, N(H)*C*Me$_3$, **7**), 53.6 (d, $^2J_{P-C}$ = 31.4 Hz, N(H)*C*Me$_3$, **6**), 58.1 (s, (tmeda-*C*H$_2$, br). ^{31}P-{^{1}H} NMR (121 MHz, C_6D_6, 25 °C): δ 104.2 (s, **6**), 107.4 (s, **7**). ^{31}P{^{1}H} NMR (121 MHz, tmeda, 25 °C, in situ spectrum): δ 107.9 (s). ^{7}Li{^{1}H} NMR (116 MHz, C_6D_6, 25 °C): δ 1.7 (s, **7**), 3.0 (s, **6**). IR (film, KBr plates): ν 3318 (NH), 1212, 1181, 1028, 966, 932, 820, 633 cm^{-1}.

Temperature-Dependent ^{31}P{^{1}H} NMR (121 MHz) Study in Toluene-d_8. 213 K. ^{31}P{^{1}H} NMR: δ 101.6 (s, **6**, 6% relative intensity), 105.4 (s, **7**, 94% relative intensity).

Table 1. Crystallographic Data and Measurement Details for 1, 3, 6, and 7

	1	3	6	7
mol formula	$C_{24}H_{60}Al_2N_4P_2$	$C_{12}H_{32}GaN_2P$	$C_{24}H_{56}Li_2N_4P_2$	$C_{18}H_{44}LiN_4P$
fw	520.66	305.09	476.55	354.48
cryst syst	monoclinic	orthorhombic	orthorhombic	monoclinic
space group	$P2_1/n$ (No. 14)	$Pca2_1$ (No. 29)	$Pbca$ (No. 61)	$P2_1/n$ (No. 14)
a, Å	12.1111(6)	17.8709(4)	9.8013(2)	8.7777(3)
b, Å	8.8057(5)	15.3128(3)	17.6699(4)	16.3693(5)
c, Å	16.1039(10)	12.4896(2)	36.0172(9)	16.1099(6)
β, deg	109.291(2)	90	90	91.278(2)
V, Å^3	1621.00(16)	3417.82(12)	6237.7(2)	2314.17(14)
Z	2	8	8	4
radiation (wavelength, Å)	Mo Kα (0.710 73)	Mo Kα (0.710 73)	Mo Kα (0.710 73)	Mo Kα (0.710 73)
μ, mm^{-1}	0.206	1.687	0.156	0.125
temp. K	123(2)	123(2)	123(2)	123(2)
D_{calcd}, g cm^{-3}	1.067	1.186	1.015	1.017
cryst dimens (mm)	0.15 × 0.08 × 0.03	0.40 × 0.25 × 0.15	0.50 × 0.30 × 0.20	0.50 × 0.40 × 0.30
$2\theta_{max}$, deg	50.0	50.0	50.0	50.0
no. of rflns rec	6965	44086	34306	9574
no. of nonequiv rflns. rec	2669	6027	5433	4071
R_{merge}	0.0667	0.0706	0.0925	0.0376
no. of params refined/restraints	154/1	290/1	295/0	220/1
R1,[a] wR2[b]	0.0428, 0.0748	0.0437, 0.1167	0.0426, 0.0996	0.0377, 0.0940
goodness of fit[c]	0.829	1.087	0.923	0.981
final max, min $\Delta\rho$, e Å^{-3}	0.241, −0.262	0.634, −0.444	0.203, −0.236	0.201, −0.368

[a] $R1 = \sum(||F_o| - |F_c||)/\sum|F_o|$ (for $I > 2\sigma(I)$). [b] $wR2 = \{\sum[w(F_o^2 - F_c^2)^2]/\sum[w(F_o^2)^2]\}^{1/2}$. [c] Goodness of fit $= \{\sum[w(|F_o^2| - |F_c^2|)^2]/(N_{observns} - N_{params})\}^{1/2}$.

253 K. $^{31}P\{^1H\}$ NMR: δ 102.8 (s, **6**, 13% relative intensity), 106.5 (s, **7**, 87% relative intensity).

298 K. $^{31}P\{^1H\}$ NMR: δ 104.5 (s, **6**, 57% relative intensity), 107.6 (s, **7**, 43% relative intensity).

333 K. $^{31}P\{^1H\}$ NMR: δ 105.5 (s, **6**, 76% relative intensity), 107.8 (s, **7**, 24% relative intensity).

[*t*-BuP(NH-*t*-Bu)N(*t*-Bu)GaCl$_2$] (8). *n*-BuLi (1.6 M in hexane, 2 mmol, 1.25 mL) was added dropwise to a solution of *t*-BuP(NH-*t*-Bu)$_2$ (2 mmol, 0.46 g) in Et_2O (15 mL) at −60 °C and warmed to ambient temperature. After the mixture was stirred for an additional 30 min the resulting clear solution was added dropwise at −78 °C to $GaCl_3$ (2 mmol, 0.35 g) dissolved in Et_2O (10 mL). The resulting solution was warmed to ambient temperature. Thereafter, all volatiles were removed in vacuo and the resulting residue dissolved in hexane (20 mL), followed by filtration. **8** was obtained as a colorless solid from the filtrate at −30 °C.

Yield: 0.56 g (75%). Mp: 103 °C. Anal. Found (calcd) for $C_{12}H_{28}Cl_2GaN_2P$ (M_r = 371.97): C, 37.87 (38.75); H, 7.41 (7.59). ^1H NMR (300 MHz, C_6D_6, 25 °C): δ 0.90 (d, $^3J_{P-H}$ = 12.5 Hz, 9H, PC*Me*$_3$), 1.10 (s, 9H, NC*Me*$_3$), 1.28 (d, $^4J_{P-H}$ = 0.5 Hz, 9H, N(H)C*Me*$_3$), 3.12 (s, 1H, N*H*). $^{13}C\{^1H\}$ NMR (74 MHz, C_6D_6, 25 °C): δ 26.0 (d, $^2J_{P-C}$ = 18.1 Hz, PC*Me*$_3$), 29.4 (d, $^3J_{P-C}$ = 6.8 Hz, N(H)C*Me*$_3$), 33.9 (d, $^3J_{P-C}$ = 6.5 Hz, NC*Me*$_3$), 34.4 (d, $^1J_{P-C}$ = 33.3 Hz, P*C*Me$_3$), 53.7 (d, $^2J_{P-C}$ = 16.5 Hz, N*C*Me$_3$), 56.9 (d, $^2J_{P-C}$ = 12.3 Hz, N(H)*C*Me$_3$). $^{31}P\{^1H\}$ NMR (121 MHz, C_6D_6, 25 °C): δ 137.7 (s). IR (film, KBr plates): ν 3239 (N−H), 1240, 1191, 1021, 957, 878, 832, 783, 757, 666 cm^{-1}.

X-ray Structure Solution and Refinement. Crystallographic data for **1**, **3**, **6**, and **7** are summarized in Table 1. Figures 1−3 and 6 show the ORTEP diagrams of the solid-state structures, including selected bond lengths and angles, of **1**, **3**, **6**, and **7**, respectively. In addition, the solid-state structure of **IV** was reinvestigated and a qualitatively better data set was obtained. Data were collected on a Nonius Kappa-CCD diffractometer. The structures were solved by direct methods (SHELXS-97)[34] and refined by full-matrix least squares on F^2 (SHELXL-97).[35] All non-hydrogen atoms were refined anisotropically and hydrogen atoms by a riding model. Empirical absorption corrections were applied for **3**.

X-ray Powder Diffraction. A glass capillary (o.d. 0.5 mm) was filled in a glovebox with a finely ground sample of as-prepared **7** and sealed. The X-ray diffraction pattern of **7** was recorded on a STOE StadiP powder diffractometer (Cu Kα_1, Ge monochromator, linear position sensitive detector (6°), 294-(1) K). An angle correction using Si as external standard was applied. The least-squares refinement[36] of 65 single-indexed lines yielded the following room-temperature lattice parameters: a = 894.25(17) pm, b = 1659.7(3) pm, c = 1629.6(3) pm, β = 91.074(10)°.

Acknowledgment. S.S. wishes to thank the Deutsche Forschungsgemeinschaft, the Fonds der Chemischen Industrie, the Bundesministerium für Bildung, Wissenschaft, Forschung und Technologie (BMBF), and Prof. E. Niecke, Universität Bonn, for financial support.

Supporting Information Available: Tables of bond distances, bond angles, anisotropic temperature factor parameters, and fractional coordinates for **1**, **3**, **6**, **7**, and **IV** and a comparison between an experimental powder X-ray diffraction pattern of **7** and the calculated pattern of **6**. This material is available free of charge via the Internet at http://pubs.acs.org.

OM0301839

(34) Sheldrick, G. M. SHELXS-97, Program for Structure Solution. *Acta Crystallogr., Sect. A* **1990**, *46*, 467.

(35) Sheldrick, G. M. SHELXL-97, Program for Crystal Structure Refinement; Universität Göttingen, Göttingen, Germany, 1997.

(36) STOE WinXPow 1.05; STOE & Cie GmbH, Darmstadt, Germany, 1999.